Interface induced out-of-plane magnetic anisotropy in magnetoelectric $BiFeO_3$-$BaTiO_3$ superlattices

Vera Lazenka, Johanna K. Jochum, Michael Lorenz, Hiwa Modarresi, Haraldur P. Gunnlaugsson, Marius Grundmann, Margriet J. Van Bael, Kristiaan Temst, and André Vantomme

Citation: Appl. Phys. Lett. **110**, 092902 (2017); doi: 10.1063/1.4977434

View online: https://doi.org/10.1063/1.4977434

View Table of Contents: http://aip.scitation.org/toc/apl/110/9

Published by the American Institute of Physics

Interface induced out-of-plane magnetic anisotropy in magnetoelectric $BiFeO_3$-$BaTiO_3$ superlattices

Vera Lazenka,[1,a),b)] Johanna K. Jochum,[2,a),b)] Michael Lorenz,[3] Hiwa Modarresi,[1] Haraldur P. Gunnlaugsson,[1] Marius Grundmann,[3] Margriet J. Van Bael,[2] Kristiaan Temst,[1] and André Vantomme[1]

[1]*KU Leuven, Instituut voor Kern- en Stralingsfysica, Celestijnenlaan 200 D, 3001 Leuven, Belgium*
[2]*KU Leuven, Laboratorium voor Vaste-Stoffysica en Magnetisme, Celestijnenlaan 200D, 3001 Leuven, Belgium*
[3]*Institut für Experimentelle Physik II, Universität Leipzig, Linnéstraße 5, D-04103 Leipzig, Germany*

(Received 21 December 2016; accepted 13 February 2017; published online 27 February 2017)

Room temperature magnetoelectric $BiFeO_3$-$BaTiO_3$ superlattices with strong out-of-plane magnetic anisotropy have been prepared by pulsed laser deposition. We show that the out-of-plane magnetization component increases with the increasing number of double layers. Moreover, the magnetoelectric voltage coefficient can be tuned by varying the number of interfaces, reaching a maximum value of 29 V/cm Oe for the $20\times BiFeO_3$-$BaTiO_3$ superlattice. This enhancement is accompanied by a high degree of perpendicular magnetic anisotropy, making the latter an ideal candidate for the next generation of data storage devices. *Published by AIP Publishing.* [http://dx.doi.org/10.1063/1.4977434]

With the ever-expanding demand for smaller, faster, and energetically more efficient data storage devices, multiferroic materials, exhibiting *ferroelectricity* and *ferromagnetism* simultaneously, are of great interest. Ferroelectric and ferromagnetic materials have been used for a long time in ferroelectric (FeRAM) and magnetic (MRAM) memory devices, respectively. In FeRAMs, the polarization is switched by an electric field, whereas in MRAMs, the magnetization is reversed by a magnetic field. However in small size devices, magnetic fields are difficult to apply locally in order to write a single bit, without influencing the neighboring ones. Introducing multiferroics in the field of spintronics makes an electric field control of the magnetic spin state possible through magnetoelectric (ME) coupling.[1,2] Intrinsic multiferroic materials are rare and almost all of them are antiferromagnetic and need low temperatures to operate.[3] The only single-phase multiferroic material exhibiting explicit magnetoelectric coupling at room temperature is $BiFeO_3$.[4] However, $BiFeO_3$ is a weak ferromagnet in a thin film form and its ME coupling is too weak to be used in an actual device.[5] Recently, strong strain-mediated ME interaction was observed in multiferroic composites and layered heterostructures.[6–9] These systems operate by coupling the magnetic and electric properties of two materials (ferroelectric and (anti-) ferromagnetic, respectively) via interfacial strain. When an electric field is applied across the sample, it induces strain in the ferroelectric component due to the inverse piezoelectric effect. This strain is mechanically transferred to the magnetic component, inducing a magnetization change through the piezomagnetic effect.[10,11]

Thin multilayered films with strong out-of-plane (OOP) magnetic anisotropy, i.e., magnetization aligned perpendicular to the film surface, are the best candidates for next-generation non-volatile memory. In such systems, there is a large energy barrier for magnetization switching, implying higher stability of the magnetization states, and lower critical current for spin-transfer torque memory devices.[12–14] The electric-field-induced magnetization reversal in a multiferroic $BiFeO_3$-$CoFe_2O_4$ composite thin film with perpendicular magnetic anisotropy (PMA) has already been demonstrated by Zavaliche *et al.*[15]

In the present work, we demonstrate the formation of perpendicular magnetic anisotropy (PMA) at the interfaces in a multiferroic magnetoelectric $BiFeO_3$-$BaTiO_3$ superlattice. The high magnetoelectric voltage coefficient values reached in the $BiFeO_3$-$BaTiO_3$ films make this multilayered system an ideal candidate for memory devices with the possibility of *tuning the magnetic and magnetoelectric states by varying the number of interfaces*.

The $BiFeO_3$-$BaTiO_3$ superlattices with nominal single layer thicknesses of 15 nm and 10 nm, respectively, and with varying number of double layers (2, 5, 10, and 20) were grown by pulsed laser deposition (PLD) from single phase $BiFeO_3$ and $BaTiO_3$ targets onto $SrTiO_3$(001) substrates at 680 °C. The $BiFeO_3$ layers were grown from a 66.7% ^{57}Fe-enriched target, which was pressed and sintered from Bi_2O_3 and Fe_2O_3 powders in stoichiometric ratio. Approximately 1.4 g $^{57}Fe_2O_3$ powder was synthesized from 1 g ^{57}Fe powder using a simple chemical route.

X-ray diffraction (XRD) 2θ-ω scans and reciprocal space maps were measured using a PANalytical X'pert PRO MRD with CuK_α radiation using a parabolic mirror and a PIXcel^{3D} array detector. From the XRD superlattice peaks, the double layer thickness for all 4 samples was found to be in the range of 21–23 nm, see Table I and supplementary material.

The magnetic order and the electronic ^{57}Fe configuration of the multilayers have been determined via conversion electron Mössbauer spectroscopy (CEMS). The Mössbauer

[a)]V. Lazenka and J. K. Jochum contributed equally to this work.
[b)]Electronic addresses: Vera.Lazenka@.kuleuven.be and johanna.jochum@kuleuven.be

TABLE I. Sample parameters deduced from the XRD and Mössbauer measurements: the layer thickness, the isomer shift at the P(B_{Hf}) peak (δ_{Bpeak}), the quadrupole shift at the P(B_{Hf}) peak (ε_{Bpeak}), the hyperfine magnetic field value at the P(B_{Hf}) peak (B_{Hfpeak}), the peak intensity ratio $I_{1(6)}$:$I_{2(5)}$:$I_{3(4)}$, and the average angle (β) between the net magnetic moment of the ^{57}Fe atoms and the incoming γ-ray.

Sample	Double layer thickness (nm)	δ_{Bpeak} (mm/s)	ε_{Bpeak} (mm/s)	B_{Hfpeak}, T	Peak intensity ratio	B (°)
20×$BiFeO_3$-$BaTiO_3$	23.2 ± 0.3	0.38 (1)	0.021 (6)	49.7 (2)	3:0.52 (3):1	28.7
10×$BiFeO_3$-$BaTiO_3$	22.1 ± 0.6	0.37 (1)	0.07 (2)	49.7 (4)	3:0.93 (3):1	37.9
5×$BiFeO_3$-$BaTiO_3$	22.8 ± 0.6	0.37 (1)	0.09 (2)	49.8 (5)	3:1.30 (4):1	44.5
2×$BiFeO_3$-$BaTiO_3$	21.1 ± 0.8	0.38 (1)	0.09 (5)	49 (2)	3:2.12 (6):1	56.4

spectra were recorded at zero magnetic field and room temperature and fitted using the Vinda software.[16] It is well known that bulk $BiFeO_3$ is a G-type antiferromagnet possessing a cycloidal spin structure with a period of 62 nm.[17] The magnetic moment gradually rotates in the plane determined by the propagation direction of the cycloid [1-10] and the polarization direction [111], which is the principal axis of the electric field gradient (EFG) tensor (Fig. 1). Any rotation of the magnetic moments by an angle θ relative to the EFG main axis results in a shift of the hyperfine energy levels, which also leads to an angular variation of the quadrupole splitting.[18,19] Hence in $BiFeO_3$, there exists a continuous distribution of spins oriented differently with respect to the principal axis of the EFG tensor. The Mössbauer spectra were fitted using the "hyperfine field distribution" model within the Vinda software. This model takes into account possible coupling between the isomer (δ) and quadrupole shift (ε) and the hyperfine field (B_{Hf}): $\delta = \delta_0 + \delta_1 B_{Hf}$ and $\varepsilon = \varepsilon_0 + \varepsilon_1 B_{Hf}$, where $\delta_1 = d\delta/dB_{Hf}$ and $\varepsilon_1 = d\varepsilon/dB_{Hf}$ are fitting variables.

Figure 2(a) shows the experimental CEMS data and fits (solid red lines) for the $BiFeO_3$-$BaTiO_3$ multilayers with varying number of interfaces. The results of the hyperfine field distributions deduced from the fit are presented in Fig. 2(b). These field distributions are characterized by only one maximum, which is the signature of the suppressed spiral cycloid in the 15 nm thin $BiFeO_3$ layers.[20] Furthermore, it can be seen that the hyperfine field distributions are asymmetric, which is most likely due to the interfacial iron which is at a position of reduced symmetry.

Table I lists the hyperfine nuclear parameters obtained from the fitting of the spectra: the hyperfine magnetic field value (a measure of the local magnetization) at the peak of the distribution (B_{Hfpeak}); the isomer shift (δ), which is determined by the Fe valence state; and the quadrupole shift (ε), which reveals the symmetry of the charge distribution around the ^{57}Fe nucleus. All spectra exhibit an asymmetric magnetic sextet with isomer shift values of 0.34–0.38 mm/s, characteristic of magnetically ordered Fe^{3+} ions in octahedral coordination. The clear asymmetry in the peak intensity in $BiFeO_3$ was observed and explained earlier by Lebeugle *et al.* It is inherent to the intrinsic anisotropy of the magnetic hyperfine interaction at a site with trigonal symmetry.[18]

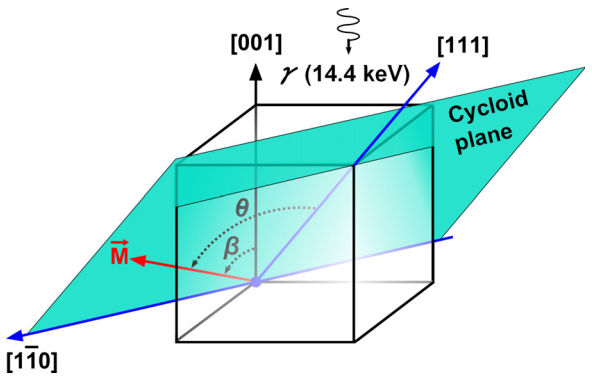

FIG. 1. Schematic view of the Mössbauer measurement geometry and the cycloid plane.

From Table I, it is clear that the number of interfaces in the $BiFeO_3$-$BaTiO_3$ superlattice does not affect the values of the hyperfine field, quadrupole, and isomer shifts. Therefore, there is no substantial difference in the electronic configurations of the ^{57}Fe atoms in all superlattices. The only parameter that gradually changes with the number of interfaces is the peak intensity ratio, which depends on the orientation of the net magnetic moment with respect to the direction of the incident γ-ray beam. The intensity ratio $I_{1(6)}$:$I_{2(5)}$:$I_{3(4)}$ between lines 1(6), 2(5), and 3(4) can be calculated using $3(1+\cos^2\beta)$:$4\sin^2\beta$:$(1+\cos^2\beta)$, where β is the angle between the net magnetic moment of the ^{57}Fe atoms and the incoming γ-ray (see Fig. 1). In the case of out-of-plane magnetic anisotropy, i.e., $\beta = 0$, the peak intensity ratio $I_{1(6)}$:$I_{2(5)}$:$I_{3(4)} = 3:0:1$. Random and in-plane (IP) orientations of the magnetic moments result in *3:2:1* and *3:4:1* ratios, respectively. As seen from Table I, the gradually increasing number of interfaces leads to PMA. When the number of $BiFeO_3$-$BaTiO_3$ double layers reaches 20, the preferential orientation of the net magnetic moment is becoming close to perpendicular to the film surface.

When varying the $BiFeO_3$ sublayer thickness rather than the double layer repetition, we found that the angle between the net magnetic moment of the ^{57}Fe atoms and the normal to the surface decreases from 47° to 33° when decreasing the layer thickness from 50 to 10 nm (results not shown here). This is additional evidence of the PMA in $BiFeO_3$/$BaTiO_3$ superlattices.

In order to further confirm the PMA development, a magnetization study of the superlattices in both in-plane (IP) and out-of-plane (OOP) geometries has been performed using SQUID magnetometry (Superconducting QUantum Interference Device, LOT-QuantumDesign MPMS-XL and MPMS3). The magnetization was measured up to fields of 7 T and a linear background has been subtracted. Since the samples were not saturated in the in-plane orientation, the data were normalized to the highest magnetization value of the corresponding loop, to allow a comparison of the in- and out-of-plane data. While the lack of saturation in the in-plane direction does not allow a quantitative analysis of

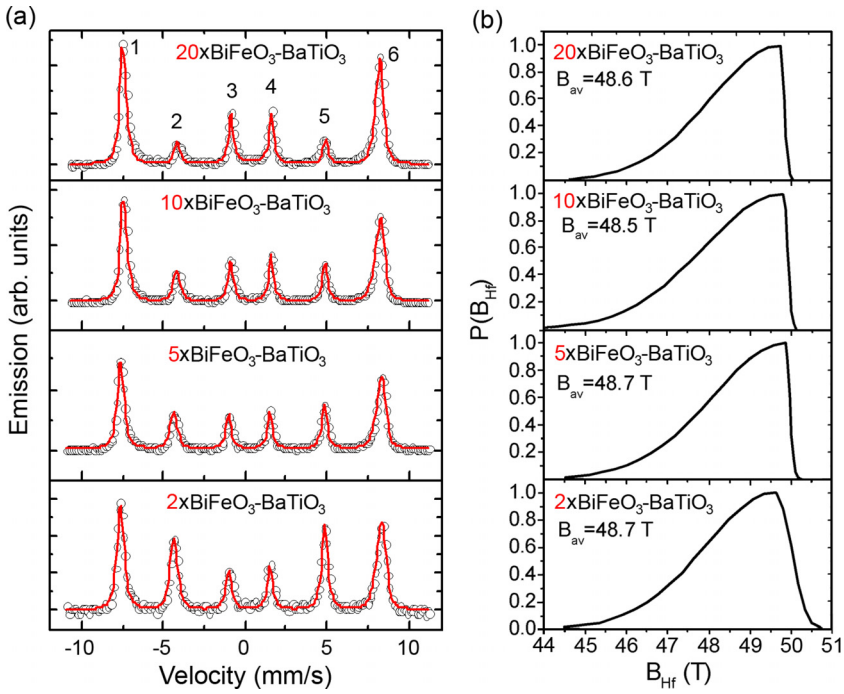

FIG. 2. (a) Conversion electron Mössbauer spectra and (b) hyperfine field distribution functions $P(B_{Hf})$ for the $BiFeO_3$-$BaTiO_3$ superlattices with different numbers of double layers. The red lines are fits. B_{av} indicates the average hyperfine field.

the magnetization data, a qualitative analysis is still possible. The measured M–H loops (Figs. 3 and S3–S6, supplementary material) confirm the ferromagnet-like behavior of the films, which also supports the suppression of the spiral cycloid in the superlattices, leading to the creation of a net magnetic moment after cycloid symmetry breakdown.[21] Figure 3 shows the perpendicular easy axis for the samples with 20 and 10 double layers, an effect that becomes less pronounced as the number of double layers is decreased. Moreover, the inset in Fig. 3 illustrates that the out-of-plane saturation field increases as the number of double layer repetitions decreases. These observations further confirm the emergence of perpendicular magnetic anisotropy in samples with an increasing number of interfaces.

The interface magnetic anisotropy in metallic multilayers has been the subject of extensive research since a long time.[14,22–25] For example, Carcia[22] studied Pd/Co and Pt/Co superlattices with an unusual perpendicular anisotropy attributed to an interfacial contribution. Sato[23] succeeded in growing Tb/Fe superlattices with interface-concentrated PMA, whose origin was attributed to the Tb-Fe pairs aligned perpendicular to the films. Recently, interface PMA has been reported in metal/oxide systems like CoFeB–MgO[14] and Fe/MgO[24,25] The enhancement of the out-of-plane magnetic moment component in Fe/MgO was explained by the anisotropic orbital magnetic moments induced by the spin-orbit interaction at the interface.[24] Based on *ab initio* calculations, Yang *et al.*[26] ascribed the large PMA at Fe/MgO interfaces

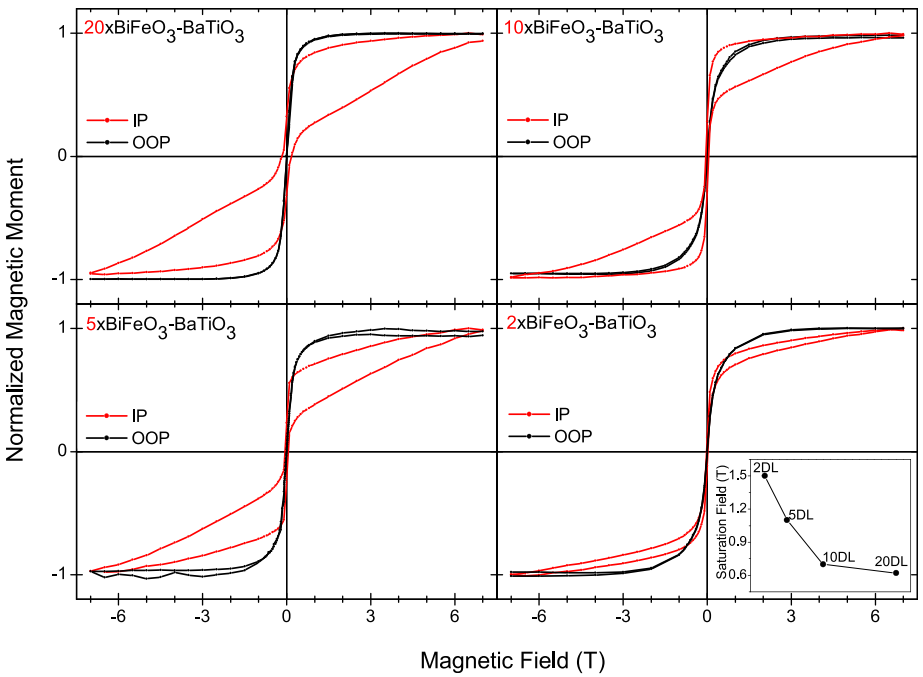

FIG. 3. Normalized out-of-plane (OOP) and in-plane (IP) magnetization curves at 300 K of the indicated superlattices, showing the emergence of a perpendicular easy axis in multilayers with a larger number of double layers. The inset shows the OOP saturation field as a function of the number of double layers.

to a combination of several factors: the degeneracy lift of out-of-plane (d_z^2, d_{xz}, and d_{yz}) $3d$ orbitals, hybridizations between d_z^2 and d_{xz} and d_{yz} $3d$ orbitals induced by spin-orbit interaction, and hybridizations between Fe-$3d_z^2$ and O-$2p_z$ orbitals at the interface. Moreover, it was also shown that in the case of a non-perfect interface (over- or underoxidized), the PMA amplitude is decreasing.[26] This is due to the disappearance of the d_z^2 hybridized states around the Fermi level in the presence or absence of an additional oxygen atom at the interface.

In the case of $BiFeO_3$-$BaTiO_3$ superlattices, we have shown that the first single layers near the substrate are strained and distorted due to the lattice mismatch.[27] These interfaces contain a number of imperfections including oxygen defects, which according to Yang *et al.*,[26] weaken the out-of-plane magnetic anisotropy. When more layers are added, the subsequent interfaces show perfect atomic arrangement with sharp atomic interfaces.[27] Therefore, we can infer that these high-quality interfaces contribute to the formation of the out-of-plane magnetic anisotropy.

To study the PMA effect on the magnetoelectric behavior of the superlattices, the ME voltage coefficient was measured as a function of external magnetic field at 300 K using the inductive AC method. More details on the method can be found in Refs. 6 and 28. The overall behavior of the ME coefficient curves for the $BiFeO_3$-$BaTiO_3$ superlattices is in agreement with our previous work.[11,29] The ME coefficient increases with increasing magnetic field and saturates around 3 T for the sample containing 20 double layers and around 1 T for the other samples (Fig. 4). The value of the ME coefficient increases with the increasing number of double layers, following the same trend as that of the out-of-plane magnetization component. This tendency is expected because of the experimental geometry: during ME measurements, the samples are positioned with their surface perpendicular to the AC and DC magnetic fields (see the inset in Fig. 4).

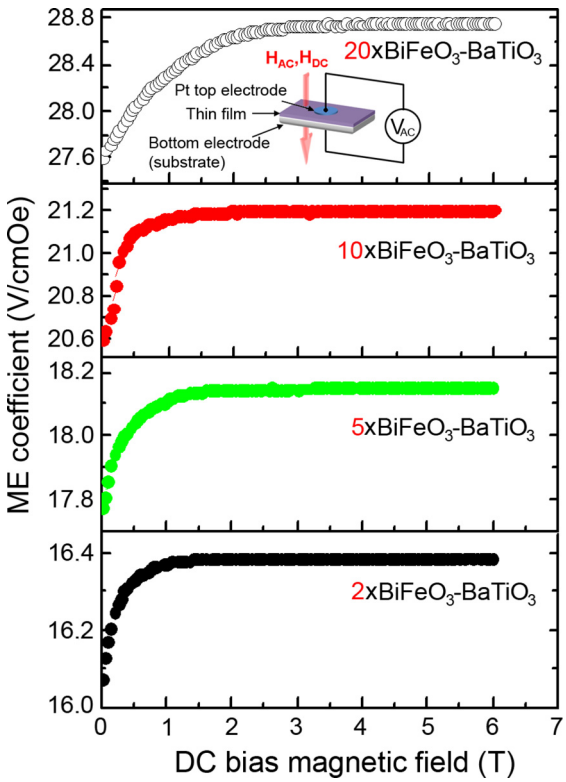

FIG. 4. Magnetoelectric coefficient as a function of DC bias magnetic field at 300 K for the $BiFeO_3$-$BaTiO_3$ superlattices with different numbers of double layers as indicated.

In conclusion, $BiFeO_3$(15 nm)-$BaTiO_3$(10 nm) superlattice structures with varying number of double layers (2, 5, 10, and 20) have been fabricated in order to study the effect of interfaces on the magnetic and magnetoelectric performance. We have demonstrated that perpendicular magnetic anisotropy is induced by the interfaces and have achieved a nearly perpendicularly magnetized $20\times$$BiFeO_3$-$BaTiO_3$ superlattice. Furthermore, the magnetization and magnetoelectric coefficient values can be tuned by varying the number of double layers. Considering the strong out-of-plane magnetic anisotropy together with its ME coupling demonstrated in this work, the $BiFeO_3$-$BaTiO_3$ superlattices can be a promising building block for future non-volatile memory devices.

See supplementary material for X-ray diffraction 2q-w scans, reciprocal space maps, and an enlarged view of the hysteresis loops.

We thank Ludwig Henderix for the synthesis of the ^{57}Fe enriched Fe_2O_3. We acknowledge the financial support from the Research Foundation Flanders (FWO), the Concerted Research Actions GOA/09/006 and GOA/14/007 of KU Leuven and the Hercules Foundation. Work at the University Leipzig was supported by the Deutsche Forschungsgemeinschaft within SFB 762 "Functionality of oxide interfaces."

[1]R. Ramesh and N. A. Spaldin, Nat. Mater. **6**, 21 (2007).
[2]M. Bibes and A. Barthélémy, Nat. Mater. **7**, 425 (2008).
[3]M. Fiebig, J. Phys. D: Appl. Phys. **38**, R123 (2005).
[4]J. T. Heron, J. L. Bosse, Q. He, Y. Gao, M. Trassin, L. Ye, J. D. Clarkson, C. Wang, J. Liu, S. Salahuddin, D. C. Ralph, D. G. Schlom, J. Íñiguez, B. D. Huey, and R. Ramesh, Nature **516**, 370 (2014).
[5]J. Wang, J. B. Neaton, H. Zheng, V. Nagarajan, S. B. Ogale, B. Liu, D. Viehland, V. Vaithyanathan, D. G. Schlom, U. V. Waghmare, N. A. Spaldin, K. M. Rabe, M. Wuttig, and R. Ramesh, Science **299**, 1719 (2003).
[6]M. Lorenz, V. Lazenka, P. Schwinkendorf, F. Bern, M. Ziese, H. Modarresi, A. Volodin, M. J. Van Bael, K. Temst, A. Vantomme, and M. Grundmann, J. Phys. D: Appl. Phys. **47**, 135303 (2014).
[7]A. Kulkarni, K. Meurisch, I. Teliban, R. Jahns, T. Strunskus, A. Piorra, R. Knöchel, and F. Faupel, Appl. Phys. Lett. **104**, 022904 (2014).
[8]H. Greve, E. Woltermann, H.-J. Quenzer, B. Wagner, and E. Quandt, Appl. Phys. Lett. **96**, 182501 (2010).
[9]M. Fiebig, T. Lottermoser, D. Meier, and M. Trassin, Nat. Rev. Mater. **1**, 16046 (2016).
[10]Y. Wang, J. Hu, Y. Lin, and C.-W. Nan, NPG Asia Mater. **2**, 61 (2010).
[11]V. Lazenka, M. Lorenz, H. Modarresi, M. Bisht, R. Rüffer, M. Bonholzer, M. J. Van Bael, A. Vantomme, and K. Temst, Appl. Phys. Lett. **106**, 082904 (2015).
[12]A. D. Kent, Nat. Mater. **9**, 699 (2010).
[13]T. Kishi, H. Yoda, T. Kai, T. Nagase, E. Kitagawa, M. Yoshikawa, K. Nishiyama, T. Daibou, M. Nagamine, M. Amano, S. Takahashi, M. Nakayama, N. Shimomura, H. Aikawa, S. Ikegawa, S. Yuasa, K. Yakushiji, H. Kubota, A. Fukushima, M. Oogane, T. Miyazaki, and K. Ando, "Lower-current and fast switching of a perpendicular TMR for high speed and high density spin-transfer-torque MRAM," Tech. Dig. - IEEE Int. Electron Devices Meet. **2008**, 1–4.
[14]S. Ikeda, K. Miura, H. Yamamoto, K. Mizunuma, H. D. Gan, M. Endo, S. Kanai, J. Hayakawa, F. Matsukura, and H. Ohno, Nat. Mater. **9**, 721 (2010).
[15]F. Zavaliche, T. Zhao, H. Zheng, F. Straub, M. P. Cruz, P.-L. Yang, D. Hao, and R. Ramesh, Nano Lett. **7**, 1586 (2007).

[16]H. P. Gunnlaugsson, "Spreadsheet based analysis of Mössbauer spectra," Hyperfine Interact. **237**, 79 (2016).
[17]I. Sosnowska, T. P. Neumaier, and E. Steichele, J. Phys. C: Solid State Phys. **15**, 4835 (1982).
[18]D. Lebeugle, D. Colson, A. Forget, M. Viret, P. Bonville, J. F. Marucco, and S. Fusil, Phys. Rev. B **76**, 024116 (2007).
[19]D. Sando, A. Agbelele, D. Rahmedov, J. Liu, P. Rovillain, C. Toulouse, I. C. Infante, A. P. Pyatakov, S. Fusil, E. Jacquet, C. Carrétéro, C. Deranlot, S. Lisenkov, D. Wang, J.-M. Le Breton, M. Cazayous, A. Sacuto, J. Juraszek, A. K. Zvezdin, L. Bellaiche, B. Dkhil, A. Barthélémy, and M. Bibes, Nat. Mater. **12**, 641 (2013).
[20]V. V. Pokatilov and V. S. Pokatilov, Solid State Phenom. **152–153**, 93 (2009).
[21]F. Bai, J. Wang, M. Wuttig, J. Li, N. Wang, A. P. Pyatakov, A. K. Zvezdin, L. E. Cross, and D. Viehland, Appl. Phys. Lett. **86**, 032511 (2005).
[22]P. F. Carcia, J. Appl. Phys. **63**, 5066 (1988).
[23]N. Sato, J. Appl. Phys. **59**, 2514 (1986).
[24]J. Okabayashi, J. W. Koo, H. Sukegawa, S. Mitani, Y. Takagi, and T. Yokoyama, Appl. Phys. Lett. **105**, 122408 (2014).
[25]J. W. Koo, S. Mitani, T. T. Sasaki, H. Sukegawa, Z. C. Wen, T. Ohkubo, T. Niizeki, K. Inomata, and K. Hono, Appl. Phys. Lett. **103**, 192401 (2013).
[26]H. X. Yang, M. Chshiev, B. Dieny, J. H. Lee, A. Manchon, and K. H. Shin, Phys. Rev. B **84**, 054401 (2011).
[27]M. Lorenz, V. Lazenka, P. Schwinkendorf, M. J. Van Bael, A. Vantomme, K. Temst, M. Grundmann, and T. Höche, Adv. Mater. Interfaces **3**, 1500822 (2016).
[28]V. V. Lazenka, G. Zhang, J. Vanacken, I. I. Makoed, A. F. Ravinski, and V. V. Moshchalkov, J. Phys. D: Appl. Phys. **45**, 125002 (2012).
[29]M. Lorenz, G. Wagner, V. Lazenka, P. Schwinkendorf, H. Modarresi, M. J. Van Bael, A. Vantomme, K. Temst, O. Oeckler, and M. Grundmann, Appl. Phys. Lett. **106**, 012905 (2015).